

## Auger electron emission from solid surfaces under heavy-ion bombardment

W. Schmidt, P. Müller,\* V. Brückner, F. Löffler, G. Saemann-Ischenko, and W. Schubert

*Physikalisches Institut der Universität Erlangen-Nürnberg, Erwin-Rommel-Str. 1,  
D-8520 Erlangen, West Germany*

(Received 2 September 1980; revised manuscript received 9 January 1981)

$L_{23}VV$  and  $KLL$  Auger spectra produced by 2-keV electrons, 3-MeV protons, and 0.8–2-MeV/amu  $^{16}\text{O}$ ,  $^{32}\text{S}$ , and  $^{35}\text{Cl}$  ions using solid targets of Al and Si were measured. No satellite lines of the  $L_{23}VV$  transition were observed, a result which can be explained by relaxation phenomena as an effect of the solid state. Additional structure at the high-energy side of the  $L_{23}VV$  peak can be ascribed to multiple  $L$ -shell vacancies in the initial state. The intensities of these hypersatellites are discussed within the statistical model of multiple ionization.

### I. INTRODUCTION

Investigation of x-ray emission has been used in the past to obtain information about the chemical environment of atoms. In particular much attention has been directed towards the study of environmental effects on the  $K\alpha$ -satellite structure produced by heavy-ion bombardment.<sup>1,2</sup> The satellites have been ascribed to transitions between a single-ionized inner shell and multiple-ionized outer shells. Therefore, from the intensities of the satellites in  $K\alpha$ -x-ray spectra, an apparent mean number of  $L$ -shell vacancies was determined. This number depends both on the number of vacancies produced by the impinging ion and on relaxation effects occurring in the inner atomic shells before the emission of the x-ray photon takes place. The filling up of  $L$ -shell vacancies with  $M$  electrons is one of these relaxation effects. Considering elements of the third row of the Periodic Table it was found that the apparent  $L$ -vacancy concentration depends on the chemical environment of the atom and can be correlated to the mean concentration of valence electrons.

The aim of our experiments was to investigate the influence of the environment of an atom to the emission of Auger electrons. The emission of Auger electrons from gases after heavy-ion impact has been studied intensively in the past.<sup>3–5</sup> Similar to the x-ray spectra, the ion-induced electron spectra reveal satellite lines. The large number of Auger satellite lines occur on the low-energy side of the Auger diagram lines and can not be resolved. To see whether the environment affects the Auger satellite structure we studied the spectra of solids after heavy-ion bombardment to compare

them with the Auger emission of gases. The main difference is expected to be due to relaxation phenomena as the electronic states of the outer shells involved are spread into electron bands.

For the first time we studied the  $L_{23}VV$  Auger ( $V$ =valence band) emission from Al and Si produced by electrons (2-keV), protons (3-MeV), and  $^{16}\text{O}$ ,  $^{35}\text{Cl}$ ,  $^{32}\text{S}$  ions (0.8–2-MeV/amu). The energy of the ions is beyond the maximum in the Coulomb ionization cross section for the  $L$  shell. Because of the small mean escape depth (10–50 Å) of low-energy electrons in solids, experiments of this type have to be performed with very clean surfaces. Therefore the use of UHV technology is necessary to get electron spectra representative of the material surface.

### II. EXPERIMENTAL

The experimental set up for "on-beam" electron spectroscopy consists of an UHV chamber ( $p \approx 3 \times 10^{-10}$  Torr) with a cylindrical mirror analyzer (CMA) and an electron gun (focus diameter  $\sim 5 \mu\text{m}$ ) mounted coaxially within the CMA. The energy resolution of the analyzer is  $\Delta E/E = 0.3\%$ . As samples, slices of Al and Si were used which were mounted to an  $x, y, z$ , and rotation manipulator. Prior to recording each secondary-electron spectrum the surfaces of the samples were cleaned by sputtering with 3-keV  $\text{Ar}^+$  ions. After sputtering no oxygen and carbon contamination of the surfaces could be detected using Auger spectroscopy.

Beams of protons and heavy ions are obtained from the Erlangen EN Tandem van de Graaff ac-

celerator. The current of the ion beams is typically 50–100 nA and the beam diameter on the sample is about 1 mm. The problem of windowless access from the beam line ( $p \approx 10^{-6}$  Torr) to the UHV chamber was solved by two-stage differential pumping. The angle between the direction of the ion beam and the central axis of the CMA is  $80^\circ$  and the target tilt angle with respect to the ion beam is  $40^\circ$ .

To record a spectrum, the number of electrons passing the analyzer at a fixed energy was counted. Simultaneously, the ion current to the target was integrated and after a preselected amount of charge of the primary beam had been collected the number of counted electrons was stored and the analyzer transmission energy was increased by a preselected value (typically 0.8 eV). This data acquisition procedure was controlled by a PDP 11/03 computer using standard CAMAC interfaces.<sup>6</sup> A spectrum was obtained within about 5 min.

The UHV chamber has further facilities for studying solid surfaces by means of photoelectron spectroscopy and elastic backscattering.

### III. RESULTS

Typical ion-induced secondary-electron spectra are shown in Fig. 1, where  $N(E)E$  is plotted versus the energy  $E$  of the emitted electrons.  $N(E)$  is the number of electrons per energy interval. The quantity  $N(E)E$  is directly proportional to the output of the CMA because of its constant relative-energy resolution ( $\Delta E/E = \text{const.}$ ).  $N(E)$ , which results from division of the measured spectra by  $E$ , is not shown in this figure, because in the  $N(E)E$  plot the Auger peaks, especially those at higher energies, can be more clearly distinguished from the secondary-electron background upon which they are superimposed.

In Fig. 1(a) the  $L_{23}VV$  and  $KLL$  Auger transitions can be seen. The relative intensity of the  $KLL$  transitions to the  $L_{23}VV$  transition is much smaller for excitation with  $^{16}\text{O}$  (16 MeV) than for excitation with  $p$  (3 MeV). This can be explained with the behavior of the Coulomb ionization cross section for inner shells.<sup>7</sup> At about 10 eV the spectra show the “true secondary-electron peak” which belongs to the secondary-electron background. Above this energy the background is continuously decreasing in  $N(E)$  spectra. Multiplying by  $E$  thus results in a broad maximum in the background which can be observed in Fig. 1. The position of

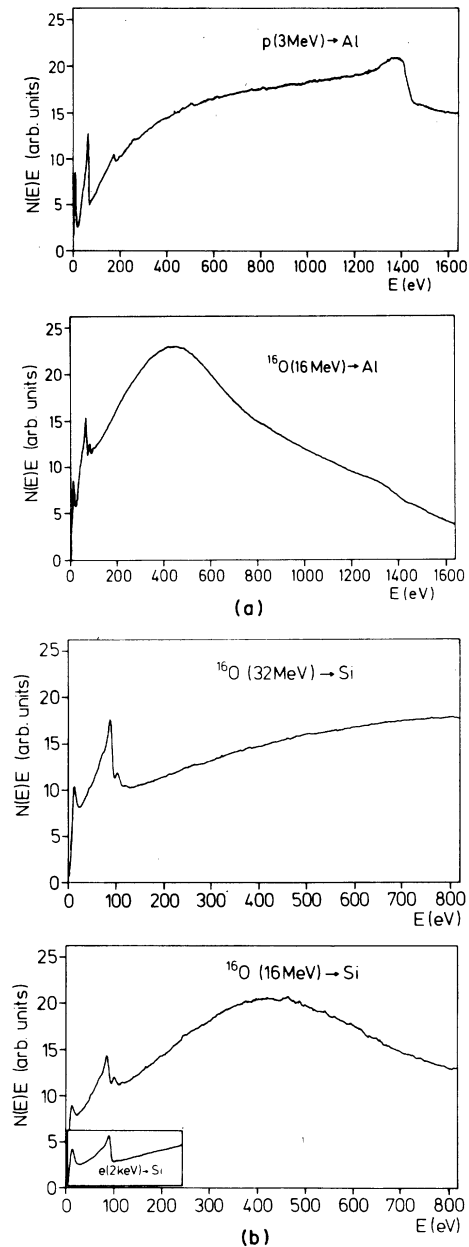


FIG. 1. (a) Secondary-electron spectra of Al bombarded with protons and oxygen ions. The peak at 66 eV is the  $L_{23}VV$  Auger transition. The  $KLL$  transitions give rise to the broad feature at 1400 eV. (b) Secondary-electron spectra of Si after bombardment with oxygen ions and electrons. The peak at 92 eV is the  $L_{23}VV$  Auger transition.

this maximum is correlated with the energy of the most energetic secondary electrons. This energy, which is about 6 keV for the 3-MeV protons and 2 keV for the 16-MeV oxygen ions, is equal to the maximum energy a projectile can transfer to a free

electron and is therefore directly proportional to the projectile energy and indirectly proportional to the projectile mass.

The ion-induced Auger transitions show features similar to the electron excited ones [Fig. 1(b)]. In comparison with collision systems using gaseous targets<sup>5</sup> [<sup>16</sup>O (27 MeV) on Ar] our spectra show the following main differences.

There is no indication of satellite lines which is a new observation. If satellite lines are present, they are only weakly excited, because shape and high-energy cutoff of the main  $L_{23}VV$  transition do not depend on the ion species used (Fig. 2) and correspond well with the electron-induced  $L_{23}VV$  transition.

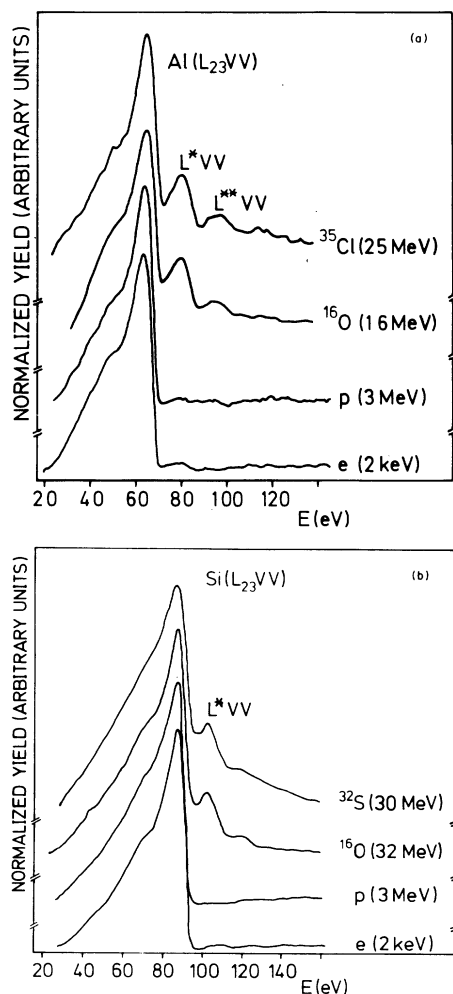


FIG. 2. Comparison of the  $L_{23}VV$  peaks in Al (a) and Si (b) after excitation with different projectiles. The peaks are normalized to equal height of the  $L_{23}VV$  transition after background subtraction. Note the increase of the  $L^*VV$  and  $L^{**}VV$  transitions in the heavy-ion spectra.

There are additional peaks at higher energies. These are also observed in electron- and proton-induced spectra, but with much smaller intensity than in heavy-ion-induced spectra.

These two results may be interpreted as follows.

#### IV. DISCUSSION

The satellite lines which are observed in similar collision systems using gaseous targets are due to multiple-ionized  $M$  shells.<sup>3</sup> Therefore, we conclude that in our spectra no  $M$ -shell vacancies are present at the time the  $L_{23}VV$  transition takes place, although  $M$ -shell vacancies were produced by the impinging ion. This is explained by the fact that  $M$  shells in Si and Al build up the valence band, so that  $M$ -shell vacancies can be filled up very fast by valence electrons. To confirm this explanation, the mean lifetime of an  $L$ -shell vacancy<sup>8</sup> [ $\tau(L_{23}) = 4 \times 10^{-15}$  sec in Ar] has to be compared to the mean lifetime of a plasmon [ $\tau(\text{plasmon}) \approx 4 \times 10^{-17}$  sec in Si],<sup>9</sup> which is a measure of the valence-shell response time. Another possible interpretation may be that the observed  $L_{23}VV$  transition is caused mainly by the primary knock-on electrons produced by the ion impact. This can be excluded primarily by the intensity ratio of the hypersatellites to the main transition, as will be discussed later.

The main difference between the heavy-ion- and electron-induced Auger peaks is the additional structure at approximately 15 eV [(15.3  $\pm$  0.3) eV in Al and (15.4  $\pm$  0.4) eV in Si] above the main  $L_{23}VV$  transition (Fig. 2). The Al spectra show several of these lines which we call  $L^*VV$ ,  $L^{**}VV$ , . . . . In the electron-excited spectra these structures are very weak. In the past two different interpretations were proposed.<sup>10</sup>

(1) The  $L^*VV$  and  $L^{**}VV$  peaks are caused by plasmon absorption. The energies of bulk (surface) plasmons measured are 17 eV (12.0 eV) in Si and 15.3 eV (10.8 eV) in Al.

(2) The projectile produces multiple ionization of the  $L$  shell. In this case the energy of the Auger transition is also increased. The peaks labeled by  $L^*VV$ ,  $L^{**}VV$  are then hypersatellites. For the free-atom case the energies of multiple-ionized atoms were calculated with a Hartree-Fock program.<sup>11</sup> We obtained an increase between the  $L_{23}MM$  and the  $L_{23}L_{23}L_{23}MM$  transition energy of 17.61 eV in Si and 15.66 eV in Al.

In our opinion the second explanation is more likely, because the relative intensity of the  $L^*VV$

peak to the  $L_{23}VV$  peak increases strongly from electron or proton excitation to heavy-ion excitation. Furthermore, the plasmon gain is caused by the intrinsic plasmons,<sup>12</sup> which are created by relaxation effects after the inner-shell vacancy has been produced. Therefore, plasmon gain should not depend on the type of the projectile which produces the vacancy.

To confirm the hypersatellite hypothesis quantitatively we determined from our spectra the quantity  $\langle l \rangle_{\text{expt}}$  defined by<sup>13</sup>

$$\langle l \rangle_{\text{expt}} = \frac{I(LVV) + 2I(L*VV) + 3I(L**VV)}{I(LVV) + I(L*VV) + I(L**VV)}.$$

$I(LVV)$ , . . . , is the integral of the  $LVV$ , . . . , transition obtained from the spectra after background subtraction. Therefore,  $\langle l \rangle_{\text{expt}}$  is the average  $L$ -shell vacancy concentration at the time of the Auger transition.<sup>13</sup> As a typical value we obtain from our measurements  $\langle l \rangle_{\text{expt}} = 1.25$  for the impact of  $^{16}\text{O}$  (30 MeV) on Al. Assuming that  $\langle l \rangle_{\text{expt}}$  is determined by the primary arrangement of  $L_{23}$  vacancies produced by the impinging ion and that the fluorescence yield of this shell is negligible, we compare  $\langle l \rangle_{\text{expt}}$  with

$$\langle l \rangle_{\text{theor}} = \frac{\sigma_{1L} + 2\sigma_{2L} + 3\sigma_{3L}}{\sigma_{1L} + \sigma_{2L} + \sigma_{3L}}.$$

$\sigma_{mL}$  is the cross section for production of  $m$  vacancies in the  $L$  shell. Differences between  $L$  subshells were neglected.

To calculate  $\sigma_{mL}$  we used the statistical model for multiple ionization,<sup>14</sup> which was successful in describing the intensities of  $K\alpha$ -x-ray satellite lines after excitation with fast ions.<sup>15</sup> Let  $P_{mL}(b)$  represent the probability that a projectile with impact parameter  $b$  produces  $m$   $L$  vacancies, then  $\sigma_{mL}$  is given by

$$\sigma_{mL} = \int_0^{\infty} P_{mL}(b) 2\pi b \, db.$$

The probabilities for multiple ionization are given by the binominal formula

$$P_{mL}(b) = \binom{8}{m} [p_L(b)]^m [1 - p_L(b)]^{8-m},$$

where  $p_L(b)$  is the probability for producing one  $L$  vacancy.

There exist several calculations from which the function  $p_L(b)$  can be taken. But for heavy projectiles like O ions all these calculations overestimate the value of  $p_L(b)$  for zero impact parameter, which can be drawn from the relative intensities of  $K\alpha$ -x-ray satellite lines.<sup>15</sup> To determine  $\langle l \rangle_{\text{theor}}$

we used  $p_L(0)$  from experimental  $K\alpha$ -x-ray satellite data<sup>16</sup> and normalized the impact parameter dependent-ionization probability computed with the binary-encounter approximation<sup>17</sup> (BEA) to this value. Therefore, a possible failure of the BEA in the present case may be not so serious. This procedure yielded  $\langle l \rangle_{\text{theor}} = 1.39$  for  $^{16}\text{O}$  (30 MeV) on Al. For the collision system  $p$  (3 MeV) on Al the  $p_L(b)$  calculated with the BEA could be used, because for light projectiles the BEA is in good agreement with experiment.<sup>16</sup> We obtained  $\langle l \rangle_{\text{theor}} = 1.01$  for  $p$  (3 MeV) on Al. To see whether our estimation depends on the BEA calculations we also used SCA (semiclassical approximation) tables<sup>18</sup> for  $p_L(b)$ . The  $p_L(b)$  from these tables was also normalized to the experimentally determined value<sup>16</sup>  $p_L(0) = 0.33$  for  $^{16}\text{O}$  (30 MeV) on Al. The result for the average  $L$ -shell vacancy concentration is  $\langle l \rangle_{\text{theor}} = 1.45$ . Thus, one can state that BEA and SCA yield almost the same value for  $\langle l \rangle_{\text{theor}}$ . This is due to the fact that the models for calculating Coulomb ionization cross sections are in good agreement, even for  $L$  shells, if the ratio of the projectile velocity to the mean velocity of the bound electron is larger than one.<sup>7</sup> Therefore, within the framework of the statistical model, the  $K\alpha$ -x-ray emission data are consistent with the results of our  $L$ -shell Auger spectra, though the latter depend on a much wider range of the impact parameter.

## V. SUMMARY

It may be a general property of Auger transitions involving the valence or conduction bands of solids that satellite lines are of negligible intensity, even after heavy-ion excitation. This missing of satellites results in surprisingly simple spectra and suggests possible applications to analysis problems using optimum projectile-target combinations for selectively enhanced excitation of special kinds of atoms. For this purpose the use of projectiles which interact with the target atoms by means of molecular-orbital excitation may be advantageous.<sup>19</sup> The energy positions and relative intensities of the additional peaks in the ion-induced Auger spectra can be well explained by multiple ionization of the  $L$  shell (hypersatellites) with reasonable assumptions. Plasmon absorption seems to be of no importance for the enhanced intensity of the additional peaks.

## ACKNOWLEDGMENTS

We wish to thank Professor W. Mehlhorn (Universität Freiburg) and Professor K. O. Groeneveld (Universität Frankfurt) for valuable discussions and Dr. W. Menzel for performing the

Hartree-Fock calculations. We acknowledge the help of Professor J. S. Briggs and Dr. L. Kocbach (Universität Freiburg) in considering some aspects of the SCA. This work was supported by the Bundesministerium für Forschung und Technologie.

- 
- \*Present address: Technische Universität München, Physik Department E21, D-8046 Garching, West Germany.
- <sup>1</sup>R. L. Watson, A. K. Leeper, B. J. Sonobe, T. Chiao, and F. E. Jenson, *Phys. Rev. A* **15**, 914 (1977).
- <sup>2</sup>J. A. Demarest and R. L. Watson, *Phys. Rev. A* **17**, 1302 (1978), and references therein.
- <sup>3</sup>N. Stolterfoht, in *Structure and Collisions of Ions and Atoms*, edited by J. A. Sellin (Springer, New York, 1978).
- <sup>4</sup>R. Mann, Report No. PA-6-77, Gesellschaft für Schwerionenforschung mbH, Darmstadt (unpublished).
- <sup>5</sup>D. Schneider, B. M. Johnson, B. Hodge, and C. F. Moore, *Phys. Lett.* **59A**, 25 (1976).
- <sup>6</sup>P. Müller, W. Schmidt, and H. J. Trebst Annual Report, Physikalisches Institut, Erlangen; p. 159 (unpublished).
- <sup>7</sup>K. Taulbjerg, *Proceedings of the Second International Conference on Inner-Shell Ionization Phenomena, Invited Papers, 1976, Freiburg, West Germany*, edited by W. Mehlhorn and R. Brenn (Universität Freiburg, Freiburg, Germany, 1976).
- <sup>8</sup>W. Mehlhorn and D. Stahlherm, *Z. Phys.* **217**, 294 (1968).
- <sup>9</sup>R. L. Kauffman, K. A. Jamison, T. J. Gray, and P. Richard, *Phys. Rev. Lett.* **36**, 1074 (1976).
- <sup>10</sup>J. T. Grant and T. W. Haas, *Surf. Sci.* **23**, 347 (1970); L. H. Jenkins and H. F. Chung, *ibid.* **28**, 409 (1971); **26**, 649 (1971); K. Wittmaack, *ibid.* **85**, 69 (1979); *Phys. Lett.* **74A**, 197 (1979).
- <sup>11</sup>C. Froese-Fischer, *Comput. Phys. Commun.* **1**, 151 (1969); **4**, 107 (1972).
- <sup>12</sup>J. C. Fuggle, in *Electron Spectroscopy, Theory, Techniques, and Applications*, edited by C. R. Brundle and A. D. Baker (Academic, New York, 1980); J. C. Fuggle, *J. Phys. F* **7**, L81 (1977).
- <sup>13</sup>C. Schmiedekamp, B. L. Doyle, T. J. Gray, R. K. Gardner, K. A. Jamison, and P. Richard, *Phys. Rev. A* **18**, 1892 (1978).
- <sup>14</sup>J. M. Hansteen and O. P. Mosebekk, *Phys. Rev. Lett.* **29**, 1361 (1972).
- <sup>15</sup>R. L. Kauffman, J. H. McGuire, P. Richard, and C. F. Moore, *Phys. Rev. A* **8**, 1233 (1973).
- <sup>16</sup>P. Richard, in *Atomic Inner Shell Processes*, edited by B. Crasemann (Academic, New York, 1975).
- <sup>17</sup>J. H. McGuire and P. Richard, *Phys. Rev. A* **3**, 1374 (1973).
- <sup>18</sup>J. M. Hansteen, O. M. Johnsen, and L. Kocbach, *At. Data Nucl. Data Tables* **15**, 305 (1975). We had a helpful discussion with L. Kocbach about the applicability of the tables.
- <sup>19</sup>K. O. Groeneveld, R. Mann, W. Meckbach, and R. Spohr, *Vacuum* **25**, 9 (1974).